

# Characterization of transient resonances in extreme-mass-ratio-inspirals

Robert H. Cole,<sup>\*</sup> Christopher P.L. Berry,<sup>†</sup> Priscilla Cañizares,<sup>‡</sup> and Jonathan R. Gair<sup>§</sup>

*Institute of Astronomy, Madingley Road, Cambridge, CB3 0HA, United Kingdom*

(Dated: September 5, 2013)

PACS numbers: 04.25.Nx, 04.30.-w, 04.70.-s, 98.62.Js

## I. INTRODUCTION

In the prologue to his classic monograph, Chandrasekhar [1] celebrates the simplicity of black holes (BHs). The Kerr solution is defined by just two parameters: mass and spin. Despite the baldness of the BH metrics, great intricacies manifest in their properties. This is made evident when a second body is introduced. The two-body problem in general relativity (GR) is well studied. It is of paramount importance for gravitational wave (GW) astronomy, where binary systems are the dominant source of radiation. Correctly modelling the dynamics of these systems is necessary to interpret and extract information from gravitational waveforms.

We have made progress in understanding the general relativistic two-body problem in recent years. Bodies of comparable mass can be studied using numerical relativity. Rapid advances in this field have been made following breakthroughs in 2005 [2–4]. These simulations shall allow us to understand BH–BH mergers. Stellar-mass BH mergers are targets for ground-based GW detectors, such as the currently mid-upgrade LIGO [5] and Virgo [6], and the in-construction Kagra [7]. Massive BH mergers, expected to be the result of galaxy mergers, are potential sources for a space-borne detector such as eLISA [8]. Systems of unequal masses are more challenging to evolve numerically as they complete a larger number of orbits and it is necessary to resolve two different scales. Calculations can instead be performed perturbatively. The paradigm unequal mass system has a stellar-mass BH orbiting a massive black hole. These extreme-mass-ratio inspirals produce GWs that are a promising signal for space-borne detectors [9]. Despite being well-studied there still remain open questions.

In the case of extreme-mass-ratio systems, efforts are concentrated on understanding the gravitational self-force [10, 11]. In the test particle limit the smaller body follows an exact geodesic of the BH’s spacetime. Including the effects of the smaller body’s finite mass, the background spacetime is perturbed. This back-reaction from this deformation alters the small body’s orbital trajectory, and can be modelled as a self-force that moves the body from its geodesic. The self-force is commonly di-

vided into two pieces, dissipative and conservative. The former encapsulates the slow decay of the orbital energy and angular momentum, constants of the motion in the test particle limit, through radiation. The latter shifts the orbital phases inducing precession. The dissipative piece is time-asymmetric and has the larger effect on the evolution of the orbital phase; the conservative piece is time-symmetric and has a smaller influence on the on the phase although this can accumulate over many orbits. Being able to accurately model the influence of the self-force shall allow us to create accurate waveform models.

Flanagan and Hinderer [12] highlighted a previously overlooked phenomenon that occurs in the general relativistic two-body problem, that of transient resonances. Geodesic orbits in GR have three associated frequencies: the radial frequency  $\Omega_r$ , the polar frequency  $\Omega_\theta$  and the azimuthal frequency  $\Omega_\phi$ . The first two describe libration and the third rotation (except in the case of polar orbits where  $\Omega_\theta$  also describes rotation) [13]. In the weak-field limit these all tend towards the Keplerian frequency; in the strong-field  $\Omega_r < \Omega_\theta < \Omega_\phi$ , and they may differ significantly. For extreme-mass-ratio systems, the evolution time-scale is much longer than the orbital period such that the motion of the smaller body is approximately geodesic over orbital time-scales. The evolution of the orbit can be approximated as a series of geodesics using the osculating element formalism [14, 15]. During this evolution, the frequencies may become commensurate. Resonances occur when the radial and polar frequencies are rational multiples of each other:

$$\nu = \frac{\Omega_r}{\Omega_\theta} = \frac{n_\theta}{n_r}, \quad (1)$$

where  $n_r$  and  $n_\theta$  are integers (with no common factors). The azimuthal motion is not important because of the axisymmetry of the background spacetime. During resonance, terms in the self-force that usually average to zero can combine coherently, significantly impacting the motion [16].

Geodesic motion in Kerr spacetime can be described by use of the action–angle formalism [13]. We shall consider a body of mass  $\mu$  orbiting a BH of mass  $M$ , with  $\eta = \mu/M \ll 1$ , and describe the motion in the directions of the standard Boyer–Lindquist coordinates using generalised angle variables  $q_\alpha = \{q_t, q_r, q_\theta, q_\phi\}$  [17]. We denote the integrals of the geodesic motion, the generalised action variables, by  $J_\alpha$ . These are some combination of the energy per unit mass  $E$ , the axial angular momentum

<sup>\*</sup> rhc2@ast.cam.ac.uk

<sup>†</sup> cplb2@ast.cam.ac.uk

<sup>‡</sup> pcm@ast.cam.ac.uk

<sup>§</sup> jgair@ast.cam.ac.uk

per unit mass  $L_z$  and the Carter constant per unit mass squared  $Q$  [18]. The system evolves following [12]

$$\frac{dq_\alpha}{d\lambda} = \omega_\alpha(\mathbf{J}) + \eta g_\alpha^{(1)}(q_r, q_\theta, \mathbf{J}) + \mathcal{O}(\eta^2), \quad (2a)$$

$$\frac{dJ_\alpha}{d\lambda} = \eta G_\alpha^{(1)}(q_r, q_\theta, \mathbf{J}) + \mathcal{O}(\eta^2), \quad (2b)$$

where  $\lambda$  is Mino time [19], and the forcing functions  $g_\alpha^{(1)}$  and  $G_A^{(1)}$  originate from the first-order self-force. At zeroth order in the mass ratio we recover the limit of purely geodesic motion: the integrals of the motion are actually constants and the angle variables evolve according to their associated frequencies  $\omega_\alpha$ .

The leading order dissipative correction to geodesic motion is calculated following the adiabatic prescription [17]: by dropping the forcing term  $g_\alpha^{(1)}$  (and all higher order terms) and replacing the the forcing term  $G_\alpha^{(1)}$  with its average over the 2-torus parametrized by  $q_r$  and  $q_\theta$   $\langle G_\alpha^{(1)} \rangle_{q_r, q_\theta}$  [20]. For most orbits this is sufficient,  $G_\alpha^{(1)}$  is given by its average value plus a rapidly oscillating component [21]. However, this averaging fails when the ratio of frequencies is the ratio of integers. In this case the trajectory does not ergodically fill the 2-torus but instead traces out a 1-dimensional subspace.<sup>1</sup> There are then contributions to the self-force that no longer average out beyond  $\langle G_A^{(1)} \rangle_{q_r, q_\theta}$ . Intuitively, we expect that this effect is more important for ratios of small integers as when the integers are large, the orbit comes close to all points on the 2-torus.

In this work we seek to characterise the importance of these resonances for the purposes of modelling extreme-mass-ratio inspirals. This requires calculating the impact that passing through a resonance has on the orbital evolution and discovering for which resonances this is significant.

We use geometric units with  $G = c = 1$  throughout. We always use  $M$  for the mass of the central massive BH and  $a$  as the spin parameter. We also use the dimensionless spin  $a_* \equiv a/M$ ; we take the convention that  $0 \leq a_* < 1$ .

## II. PROBLEM FORMULATION

### A. Kerr geodesics

The evolution of an extreme-mass-ratio ( $\eta \ll 1$ ) system is slow. Instantaneously, the motion of the orbiting mass can be described as geodesic, with the integrals of the motion changing on time-scales of many orbital periods. We analyse the behaviour of resonances with the osculating element framework, where the trajectory is described

by a sequence of geodesics which each match onto the motion at a particular instance. It is therefore necessary to develop an understanding of the Kerr geodesics.

The geodesic equations may be written as [1, 18]

$$\frac{dt}{d\lambda} = a(L_z - aE \sin^2 \theta) + \frac{r^2 + a^2}{\Delta} \mathcal{T}, \quad (3a)$$

$$\frac{dr}{d\lambda} = \pm \sqrt{V_r}, \quad (3b)$$

$$\frac{d\theta}{d\lambda} = \pm \sqrt{V_\theta}, \quad (3c)$$

$$\frac{d\phi}{d\lambda} = \frac{L_z}{\sin^2 \theta} - aE + \frac{a}{\Delta} \mathcal{T}, \quad (3d)$$

where  $\Delta = r^2 - 2Mr + a^2$ ; the signs of the  $r$  and  $\theta$  equations can be chosen independently, and we have introduced potentials

$$\mathcal{T} = E(r^2 + a^2) - aL_z, \quad (4a)$$

$$V_r = \mathcal{T}^2 - \Delta[r^2 + (L_z - aE)^2 + Q], \quad (4b)$$

$$V_\theta = Q - \cos^2 \theta \left[ a^2(1 - E^2) + \frac{L_z^2}{\sin^2 \theta} \right]. \quad (4c)$$

As an affine parameter we have used Mino time which is related to the proper time  $\tau$  by [19]

$$\tau = \int r^2 + a^2 \cos^2 \theta d\lambda. \quad (5)$$

Using Mino time allows us to decouple the  $r$  and  $\theta$  motions.

We only consider bound motion [23]. The radial motion covers a range  $r_p \leq r \leq r_a$  where the turning points are the periapsis  $r_p$  and apoapsis  $r_a$ . Drawing upon Keplerian orbits we parametrize the motion using

$$r = \frac{pM}{1 + e \cos \psi}, \quad (6)$$

introducing eccentricity  $e$ , (dimensionless) semilatus rectum  $p$  and relativistic anomaly  $\psi$  [24, 25]. While  $r$  oscillates between its maximum and minimum values,  $\psi$  increases secularly increasing by  $2\pi$  across an orbit. The polar motion covers a range  $\theta_- \leq \theta \leq \pi - \theta_-$ . We also parametrize this motion in terms of an angular phase  $\chi$ , according to [26]

$$\cos \theta = \cos \theta_- \cos \chi. \quad (7)$$

While  $\psi$  and  $\chi$  are  $2\pi$  periodic they are not the canonical action-angle variables [27]; they are, however, easy to work with.

The geodesic motion can equally be described by  $\{E, L_z, Q\}$  or  $\{p, e, \theta_-\}$  [27]. Converting between them requires finding the solutions of  $V_r = 0$  and  $V_\theta = 0$ . We employ a slightly different parameter set of  $\{p, e, \iota\}$  where we have introduced the inclination [28, 29]

$$\tan \iota = \frac{\sqrt{Q}}{L_z}. \quad (8)$$

<sup>1</sup> For illustrations, see Grossman, Levin and Perez-Giz [22].

This is  $0 \leq \iota < \pi/2$  for prograde orbits and  $\pi/2 < \iota \leq \pi$  for retrograde orbits. Equatorial orbits ( $\theta_- = \pi/2$ ) have  $\iota = 0$  or  $\pi$  and polar orbits ( $\theta_- = 0$ ) have  $\iota = \pi/2$ . While formulae exist for conversion between the different parameters, these are complicated and un insightful, so we do not reproduce them here.<sup>2</sup>

## B. Orbital resonances

The radial and polar orbital periods in Mino time are given by

$$\Lambda_r = 2 \int_{r_p}^{r_a} \frac{1}{\sqrt{V_r}} dr = \int_{-\pi}^{\pi} \frac{d\lambda}{d\psi} d\psi, \quad (9a)$$

$$\Lambda_\theta = 4 \int_{\theta_-}^{\pi/2} \frac{1}{\sqrt{V_\theta}} d\theta = \int_{-\pi}^{\pi} \frac{d\lambda}{d\chi} d\chi. \quad (9b)$$

The orbital frequencies are thus

$$\Upsilon_r = \frac{2\pi}{\Lambda_r}, \quad \Upsilon_\theta = \frac{2\pi}{\Lambda_\theta}. \quad (10)$$

The geodesic equations for coordinate time  $t$  and azimuthal angle  $\phi$  are just functions of  $r$  and  $\theta$ , hence their evolutions can be expressed as Fourier series [25]

$$\frac{dt}{d\lambda} = \sum_{k_r, k_\theta} T_{k_r, k_\theta} \exp[-i(k_r \Upsilon_r + k_\theta \Upsilon_\theta) \lambda], \quad (11a)$$

$$\frac{d\phi}{d\lambda} = \sum_{k_r, k_\theta} \Phi_{k_r, k_\theta} \exp[-i(k_r \Upsilon_r + k_\theta \Upsilon_\theta) \lambda]. \quad (11b)$$

The  $(0, 0)$  coefficients in these series give the average secular rate of increase of these quantities. We define

$$\Gamma = T_{0,0}, \quad \Upsilon_\phi = \Phi_{0,0} \quad (12)$$

to act as Mino time frequencies. We can now convert to coordinate time frequencies with

$$\Omega_r = \frac{\Upsilon_r}{\Gamma}, \quad \Omega_\theta = \frac{\Upsilon_\theta}{\Gamma}, \quad \Omega_\phi = \frac{\Upsilon_\phi}{\Gamma}. \quad (13)$$

Transient resonances occur when the radial and poloidal motions are commensurate, when

$$\nu = \frac{\Upsilon_r}{\Upsilon_\theta} = \frac{\Omega_r}{\Omega_\theta} = \frac{n_\theta}{n_r} \quad (14)$$

is the ratio of small integers. At this point any Fourier series like those in (11b) goes from being an expansion in two frequencies to being an expansion in a single frequency [30].

On resonance, the radial and polar motions are locked together such that we could express one as a function of

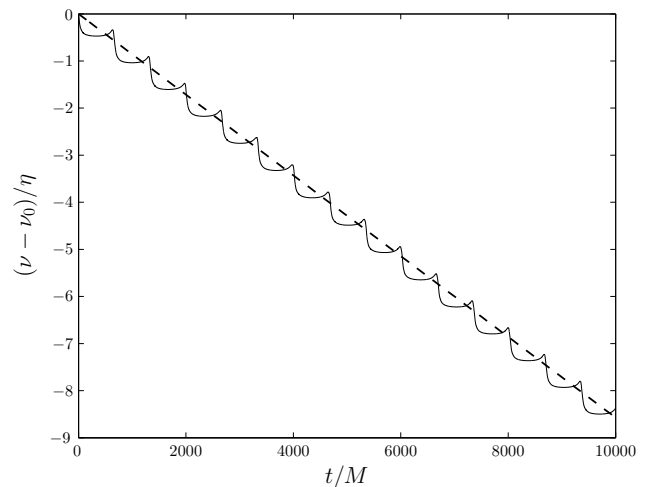


FIG. 1. Evolution of the frequency ratio  $\nu$  under both adiabatic (solid line) and instantaneous evolutions. The two coincide at  $t = 0$  when  $\nu = \nu_0$ . The behaviour is general, cf. figure 27 of Arnold [21]. In this particular example,  $\nu_0 \simeq 0.685$ ,  $\eta = 10^{-6}$  and  $a_* = 0.9$ , the initial orbital parameters are  $p = 10$ ,  $e = 0.7$  and  $\cos \iota = 0.2$ ; there are no significant resonances in the plotted span. As a reference for the time-span, the azimuthal orbital period is  $T_\phi \simeq 432M$ .

the other. For a general non-resonant orbit there is no fixed correlation between two coordinates. After a sufficiently long time, the trajectory comes arbitrarily close to every point in the range of motion (with  $r_p \leq r \leq r_a$  and  $\theta_- \leq \theta \leq \pi - \theta_-$ ); on account of the orbital precession, the whole space is densely covered. This does not happen on resonance, as the trajectory keeps cycling over the same path. The points visited are controlled by the relative phases of the  $r$  and  $\theta$  motions. To represent this, we use the  $r$  phase at the  $\theta$  turning point  $\psi_{\theta_-} = \psi(\chi = 0)$ . Varying  $\psi_{\theta_-}$  across its full range allows every point in the range of motion to be reached. Hence averaging over all values of  $\psi_{\theta_-}$  for a resonant orbit is equivalent to averaging over the  $\psi$ - $\chi$  2-torus for non-resonant orbits.

One might be concerned about the nature of resonances following the inclusion of the self-force: true geodesic motion only exists at zeroth order in  $\eta$  and, while it is a good approximation over short time-scales, for small  $\eta$  there is a small disparity. The conservative piece of the self-force induces extra precession which leads to a slight shift in the orbital frequencies [31].<sup>3</sup> The dissi-

<sup>2</sup> In practice we find turning points numerically.

<sup>3</sup> The Kolmogorov–Arnold–Moser (KAM) theorem states that when an integrable Hamiltonian (i.e., the case for motion in Kerr) is subject to a small perturbation the form of the orbits is preserved albeit slightly deformed [32, 33]. This should ensure that, in general, there are only small shifts in the orbital frequencies. However, the KAM theory only applies for sufficiently incommensurate orbits: close to resonance it does not apply [33]. This is a further reason why resonances merit an in-depth investigation.

pative piece causes the frequencies to evolve and, hence, the resonance cannot persist for multiple orbits (without some feedback coupling). In effect, we are really considering a period of time about the resonant crossing. The instantaneous orbital frequencies oscillate back and forth around their averaged values; a generic example of this behaviour is shown in Fig. 1. However, there shall be a time span when the frequencies are consistently close to being commensurate. During this time, the trajectory appears similar to a resonant trajectory, filling only a smaller region of the parameter space. It is this time period that is of interest for transient resonances [30].

### C. Self-force model

To follow the evolution of the inspiral we must have a means of modelling the self-force. In this work we use the same post-Newtonian approximation as Flanagan and Hinderer [12]. They use the first-order post-Newtonian terms of the dissipative self-force formulated in Flanagan and Hinderer [34] and the conservative force formulated in Iyer and Will [35], and Kidder [36]. Since only the first post-Newtonian terms are used, this prescription can only be of limited validity in strong fields. Both pieces of the self-force are computed assuming that the spin is small: the dissipative piece contains terms to  $\mathcal{O}(a_*^2)$  and the conservative piece to  $\mathcal{O}(a_*)$ . This is less than ideal for high spins. While this approximate self-force is not perfect, it should serve as a guide for the behaviour of the full self-force.

## III. LOCATION OF RESONANCES

The first step in studying the effect of transient resonance is to locate orbital parameters for which the frequencies are commensurate. We can calculate the frequencies and so we are left with the problem of solving  $\Omega = n_r \Omega_r - n_\theta \Omega_\theta = 0$  numerically. Fig. 2 shows the semilatus rectum, eccentricity and (cosine of the) inclination angle of the  $\nu = 2/5$  resonance surface for a BH of spin  $a_* = 0.95$ . The resonances occur at relatively small periapses, corresponding to regions of strong-field gravity. Similar resonance surfaces can be found for other spin values and for other resonances. When considering the full parameter set of  $\{p, e, \iota, a_*, \nu\}$  it is apparent that the search for resonances becomes expensive as a consequence of the dimensionality. It is therefore useful to have a guide of where to look. We shall attempt to build a model for the resonance plane.

Brink, Geyer and Hinderer [37] provide series expansions for the location of resonances in the limit of equatorial orbits for small spin and eccentricity. We do not follow this approach of trying to find analytic expressions for the resonance surface. The expressions become complicated when venturing away from limiting cases. Instead, we build an approximate phenomenological model

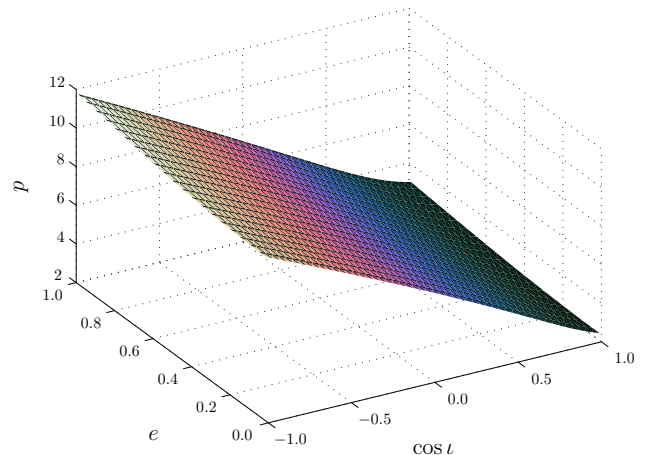


FIG. 2. Location of the  $2/5$  resonance surface for an  $a_* = 0.95$  BH in terms of orbital semilatus rectum  $p$ , eccentricity  $e$  and inclination  $\iota$ .

and fit this to the resonance plane. This should be useful for designating the region in which resonance could be expected. To locate them precisely it is necessary to solve  $\Omega = 0$  numerically; the approximate model should give a suitable starting point.

The resonant semilatus rectum for any particular spin and resonance ratio can be well approximated as

$$p(e, \iota; a_*, \nu) \simeq A \frac{1 + Be + D \cos \iota}{1 - C \exp(e)}. \quad (15)$$

The coefficients  $\{A, B, C, D\}$  depend upon the spin and the particular resonance; they can be approximated as

$$A(a_*, \nu) \simeq a_0 \frac{1 + a_1 \nu - a_2 \nu^2 - a_3 \nu a_*^2}{1 + a_4 \nu - (1 + a_4) \nu^2}, \quad (16)$$

$$B(a_*, \nu) \simeq b_0 (1 - b_1 \nu) \exp(-b_2 \nu) (1 - b_3 a_*), \quad (17)$$

$$C(a_*, \nu) \simeq c_0, \quad (18)$$

$$D(a_*, \nu) \simeq d_0 [1 - \exp(a_*)] [1 - d_1 \exp(\nu)]. \quad (19)$$

This gives us a total of 12 parameters for our fit. Whilst this may sound large, if we were fitting an expansion to quadratic order in any combination of  $\{e, \iota, a_*, \nu\}$  we would have 15 parameters.<sup>4</sup> Our optimised parameters are

$$\begin{aligned} a_0 &= 5.9854, & a_1 &= 3.4116, & a_2 &= 0.9253, \\ a_3 &= 0.1959, & a_4 &= 4.8846, & b_0 &= 0.7692, \\ b_1 &= 1.4752, & b_2 &= 1.4861, & b_3 &= 0.5974, \\ c_0 &= 0.02332, & d_0 &= 0.7968, & d_1 &= 0.3115. \end{aligned} \quad (20)$$

These were fitted for all possible resonances with  $n_r = 2-7$  as well as  $\nu = 9/10, 19/20, 49/50$  and  $99/100$ ; with MBH spins of  $a_* = 0.01-0.999$ ; for orbits with eccentricities  $e = 0.01-0.99$ , and inclinations  $\cos \iota = -0.999999-0.999999$ .

<sup>4</sup> This does not give as good a fit as our function.



Using this approximation, the maximum error in  $p$  for a given  $a_*$  and  $\nu$  is typically  $\sim 10\%$  and less than 1 in absolute terms. The relative error in the semilatus rectum is illustrated in Fig. 3. The largest fractional error is  $\sim 50\%$ , this is for  $a \rightarrow 1$  and  $\nu \rightarrow 0$ , and corresponds to small  $p$ , such that the absolute error is still small. Taking the root-mean-square across  $e$  and  $\iota$ , the fractional error for a given  $a_*$  and  $\nu$  never exceeds 9% and is typically less than 4%.

#### IV. IMPORTANCE OF RESONANCES

Having determined the location of resonances we may now address their importance. We study the enhancement of the flux of  $E$ ,  $L_z$  and  $Q$  during resonance and, equivalently, the change in the  $p$ ,  $e$  and  $\iota$ . We also investigate the dephasing in the waveform compared to a purely adiabatic evolution. This is of interest for matched filtering analysis of inspirals.

##### A. Time-scales

When analysing resonances it is useful to refer to a number of reference time-scales. We always use coordinate time  $t$  for these, as this corresponds to what is measured by an observer at infinity. Translation to Mino time can be done with an appropriate factor of  $\Gamma$ . We use the orbital period  $T$ , the evolution time-scale  $\tau_{\text{ev}}$ , the precession time-scale  $\tau_{\text{pres}}$  and the resonance time-scale  $\tau_{\text{res}}$ .

The simplest time-scales are the orbital periods  $T_r = 2\pi/\Omega_r$ ,  $T_\theta = 2\pi/\Omega_\theta$  and  $T_\phi = 2\pi/\Omega_\phi$ . These are the shortest in our set. We use  $T$  to denote a time-scale of the same order as the orbital periods.

We define the evolution time-scale as

$$\tau_{\text{ev}} = \frac{\nu}{\dot{\nu}}, \quad (21)$$

where an overdot denotes a derivative with respect to  $t$ . In general, away from resonance, we take  $\nu \equiv \Omega_r/\Omega_\theta$ . This time-scale sets the period over which there is a significant change in the frequencies. It acts as an inspiral time-scale. It is long in all cases we study,  $\tau_{\text{ev}} \sim \mathcal{O}(T/\eta)$ . It is this property which makes extreme-mass-ratio inspirals interesting, as we can follow the waveform for many cycles, accruing high signal-to-noise ratios. This is also what allows us to use the adiabatic prescription, as it means the trajectory moves slowly through different orbital parameters.

We use the precession time-scale

$$\tau_{\text{pres}}(t) = \frac{2\pi}{|\dot{\Omega}(t)|}, \quad (22)$$

with  $\Omega(t) = n_r\Omega_r(t) - n_\theta\Omega_\theta(t)$ , where the frequencies are calculated instantaneously and the integers are for

the resonance of interest. This time-scale becomes infinite exactly on resonance, but decreases as we get further from resonance, eventually becoming  $\mathcal{O}(T)$ . It measures the relative precession rate of the radial and polar motions and hence gives an indication of how long it takes to fill the entire  $\psi$ - $\chi$  2-torus.

We also use the resonance time-scale

$$\tau_{\text{res}} = \left[ \frac{2\pi}{|\langle \dot{\Omega}(0) \rangle_{q'}|} \right]^{1/2}. \quad (23)$$

Here  $\dot{\Omega}(0)$  is the rate of change of  $\Omega$  at resonance, which we take to be at  $t = 0$ . The instantaneous  $\dot{\Omega}$  depends upon the orbital phase and oscillates about its mean trend over an orbit (see Fig. 1). We are interested in the averaged behaviour, not the periodic modulations about this, which is why we use the time-average  $\langle \dot{\Omega} \rangle_{q'}$ ; here we use  $q'$  to represent a phase that varies over an orbit with period of order  $T$ . Close to resonance,  $\Omega(t)$  is well approximated by a first-order Taylor expansion, decreasing linearly with time; hence we make the approximation

$$|\langle \dot{\Omega} \rangle_{q'}| \simeq \left| \frac{\Omega(t)}{t} \right|. \quad (24)$$

The resonant time-scale should give an indication of the time over which we expect the effects of the resonance to be felt [30]. Consider the phase of the Mino time Fourier expansion on resonance; neglecting the constant, the resonant Fourier component has form

$$\varphi_{n_r, -n_\theta} \simeq (n_r \Upsilon_r - n_\theta \Upsilon_\theta) \lambda + \left( n_r \dot{\Upsilon}_r - n_\theta \dot{\Upsilon}_\theta \right) \lambda^2 + \dots \quad (25)$$

Typically, the first term is non-zero and this gives the familiar oscillation. On resonance, it is zero, leaving the next order term to govern the behaviour [12]. Only once we have moved far enough away from resonance for the first term to dominate the second do we recapture the non-resonant behaviour. The first term (translating from Mino time to coordinate time) sets  $\tau_{\text{pres}}$ , the second sets  $\tau_{\text{res}}$ .

Since we have argued that the effect of resonance can be thought of as a consequence of not densely covering the  $\psi$ - $\chi$  2-torus, we might expect that  $\tau_{\text{pres}}$ , as well as  $\tau_{\text{res}}$ , could be used for setting the resonance duration: the resonance ends once sufficient time has elapsed that the 2-torus could be filled. This is indeed the case. Let  $t_{\text{pres}}$  be the time taken to fill the torus, then

$$t_{\text{pres}} = \tau_{\text{pres}}(t_{\text{pres}}) \simeq \frac{2\pi}{|\langle \dot{\Omega}(0) \rangle_{q'} t_{\text{pres}}|}, \quad (26)$$

using (22) and substituting  $\Omega(t_{\text{pres}}) \simeq \langle \dot{\Omega} \rangle_{q'} t_{\text{pres}}$ . Rearranging and using (23) gives

$$t_{\text{pres}} \simeq \tau_{\text{res}}. \quad (27)$$

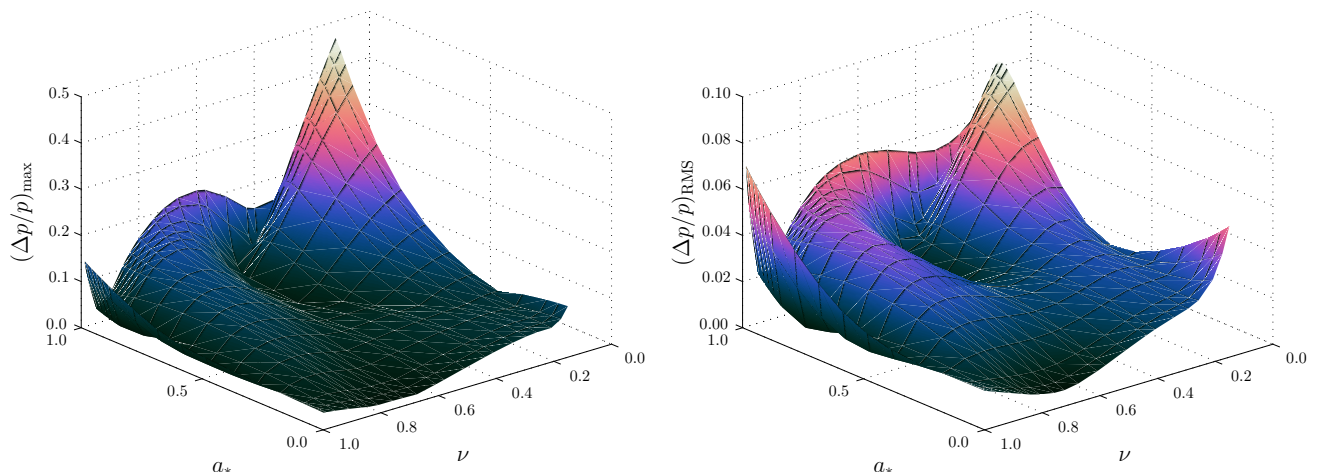


FIG. 3. Relative error in the approximate semilatus rectum compared to the accurate numerical result as a function of BH spin  $a_*$  and resonance ratio  $\nu$ . The left panel shows the maximum relative error and the right shows the root-mean-square error; in both cases we are marginalising over eccentricity and inclination.

The two time-scales are equivalent. We preferentially use  $\tau_{\text{res}}$  to denote the resonance width. It is shorter than the inspiral time-scale, but longer than an orbital period,  $\tau_{\text{res}} \sim \mathcal{O}(\eta^{1/2}\tau_{\text{ev}}) \sim \mathcal{O}(\eta^{-1/2}T)$  [12, 15]; it therefore acts as a bridge between the two time-scales [17].

Since we shall be considering Fourier decompositions, in anticipation of future results, we also define a time-scale for the  $s$ -th resonant frequency harmonic

$$\tau_{\text{res},s} = \left[ \frac{2\pi}{|s\langle\dot{\Omega}(0)\rangle_{q'}|} \right]^{1/2}. \quad (28)$$

This assumes that  $s$  is a non-zero integer.

## B. Resonance enhancement

Evolving through a resonance can lead to an enhancement (or decrement) of fluxes relative to the adiabatic prescription. After crossing the resonance region, the orbital parameters are different from those calculated from an adiabatic evolution. Flanagan and Hinderer [12] gave an expression for this deviation. If we denote the orbital parameters by  $\mathcal{I}_a = \{E, L_z, Q\}$ , then the change across resonance is

$$\Delta\mathcal{I}_a = \eta \sum_{s \neq 0} F_{a,s}^{(1)} \sqrt{\frac{2\pi}{|s\langle\dot{\Omega}\rangle_{q'}|}} \times \exp \left[ i \left( s\hat{\kappa}_0 + \frac{\pi}{4} \text{sgn } s\langle\dot{\Omega}\rangle_{q'} \right) \right]. \quad (29)$$

Here  $\hat{\kappa}_0$  is the orbital phase on resonance and  $F_{a,s}^{(1)}$  is the  $s$ -th harmonic of the first-order self-force on resonance,

defined such that<sup>5</sup>

$$\frac{d\mathcal{I}_a}{dt} = \eta \sum_s F_{a,s}^{(1)}(\mathcal{I}) \exp(isq) + \mathcal{O}(\eta^2). \quad (30)$$

A derivation is presented in Appendix A, which contains a more comprehensive explanation of the various terms. This employs matched asymptotic expansions to track the evolution through resonance, following the approach of Kevorkian [38].

The expression for the change can be understood using our expression for the resonance width, substituting in (28),

$$\Delta\mathcal{I}_a = \eta \sum_{s \neq 0} F_{a,s}^{(1)} \tau_{\text{res},s} \exp \left[ i \left( s\hat{\kappa}_0 + \frac{\pi}{4} \text{sgn } s\langle\dot{\Omega}\rangle_{q'} \right) \right]. \quad (31)$$

Schematically, this can be understood as the magnitude of the forcing function on resonance  $\sim \eta F_{a,s}$  multiplied by the time on resonance  $\sim \tau_{\text{res},s}$  and a function that varies with the phase  $\hat{\kappa}_0$ . Averaging over all values of  $\hat{\kappa}_0$  is equivalent to averaging over all values of  $\psi_{\theta_-}$ , and has the same effect as averaging over the  $\psi$ - $\chi$  2-torus; this gives an average discrepancy relative to the adiabatic evolution of

$$\langle \Delta\mathcal{I}_a \rangle_{\hat{\kappa}_0} = 0, \quad (32)$$

exactly as expected.

<sup>5</sup> Since the geodesic equations decouple in Mino time rather than coordinate time, this is true only in an average sense.

### C. Dephasing

## V. ASTROPHYSICAL IMPLICATIONS

### VI. CONCLUDING REMARKS

### ACKNOWLEDGMENTS

The authors thank Tanja Hinderer, Jeandrew Brink, Maarten van de Meent and Leor Barack for useful conversations. RHC is supported by STFC; CPLB was supported by STFC and the Cambridge Philosophical Society; PC is supported by a Marie Curie Fellowship, and JRG is supported by the Royal Society.

### Appendix A: Asymptotic solution for passage through resonance

The impact of passing through resonance on the evolution can be modelled analytically using asymptotic expansions [39]. Solutions for the motion are constructed far away from resonance and these are matched to a transition region in the vicinity of resonance [30, 40]. By comparing the matched solution, which incorporates the effects of resonance, with the results of an adiabatic evolution, it is possible to estimate the discrepancy in the orbital parameters. This determines the difference in the orbital phase between the two approaches. If this error is sufficiently small, then it is safe to ignore the effects of the resonance; however, only a small difference is needed to impact the subsequent waveform, since the error accumulates over the subsequent observation of  $\sim \mathcal{O}(\eta^{-1})$  cycles [12]. We derive formulae which can be used to calculate the discrepancy in the orbital parameters.

The following derivation is based upon the analysis of Kevorkian [38].<sup>6</sup> Small adjustments have been made to adapt to the specific problem of GW inspiral, but the general argument is unchanged.

We model the system using action-angle variables. We are only concerned with the  $r$  and  $\theta$  motions, so we have a 2-dimensional system. We perform a canonical transformation to isolate the resonant combination  $q = n_r q_r - n_\theta q_\theta$  [30]. This becomes one of the new angle variables, the other variable  $q'$  can be either  $q_r$  or  $q_\theta$  (as, on resonance, varying one necessarily changes the other). We use  $J$  as the conjugate action variable to  $q$  and  $\omega = n_r \omega_r - n_\theta \omega_\theta$  as its frequency. Similarly, we use  $J'$  as the action variable conjugate to  $q'$ . The system evolves through resonance slowly, on an evolution time-scale, so we parameterize it in terms of a slow time parameter

$$\tilde{\lambda} = \eta \lambda. \quad (\text{A1})$$

The orbits of  $q'$  proceed with the fast time  $\lambda$ ; since this is much more rapid than the evolution we are interested in, it is safe to average over it. We are not interested in the fine-grained fast oscillations caused by changes in  $q'$ . For this analysis we consider the reduced problem of evolving  $q$  and  $J$ .

At resonance  $\tilde{\lambda} = \tilde{\lambda}_*$  and  $\omega(\tilde{\lambda}_*) = 0$ . We assume that the frequency has a simple zero and can be expanded as

$$\omega(\tilde{\lambda}) = \varpi_1 (\tilde{\lambda} - \tilde{\lambda}_*) + \varpi_2 (\tilde{\lambda} - \tilde{\lambda}_*)^2 + \dots \quad (\text{A2})$$

The frequency is actually a function of the angle variables, but since these evolve with  $\tilde{\lambda}$  it is safe to write it as a function of the slow time.<sup>7</sup>

Using the slow time, the equations of motion (2a) become

$$\frac{dq}{d\tilde{\lambda}} = \frac{\omega(J)}{\eta} + \sum_s g_s^{(1)}(J) \exp(isq) + \mathcal{O}(\eta), \quad (\text{A3a})$$

$$\frac{dJ}{d\tilde{\lambda}} = \sum_s G_s^{(1)}(J) \exp(isq) + \mathcal{O}(\eta), \quad (\text{A3b})$$

where we have rewritten the forcing terms as Fourier series and adapted the forcing functions to those appropriate for  $q$  and  $J$ . We shall solve these before resonance and then match to solutions in the transition regime about resonance.

#### 1. Solution before resonance

To find a solution away from the resonance, we decompose the problem to be a function of two time-scales [40]. We use the slow time  $\tilde{\lambda}$  and, as a proxy for the fast time,

$$\Psi = \int_0^\lambda \omega(\eta\tau) d\tau = \frac{1}{\eta} \int_0^{\tilde{\lambda}} \omega(\tilde{\tau}) d\tilde{\tau}. \quad (\text{A4})$$

From this

$$\omega = \frac{d\Psi}{d\tilde{\lambda}}. \quad (\text{A5})$$

In terms of these two variables, we can build ansatz solutions

$$q(\lambda; \eta) = \Psi + q_0(\tilde{\lambda}) + \eta q_1(\Psi, \tilde{\lambda}) + \mathcal{O}(\eta^2), \quad (\text{A6a})$$

$$J(\lambda; \eta) = J_0(\tilde{\lambda}) + \eta J_1(\Psi, \tilde{\lambda}) + \mathcal{O}(\eta^2). \quad (\text{A6b})$$

We can also write a series expansion for the frequency, since it is affected by the self-force too,

$$\omega(\lambda; \eta) = \omega_0(\tilde{\lambda}) + \eta \omega_1(\tilde{\lambda}) + \mathcal{O}(\eta^2). \quad (\text{A7})$$

<sup>6</sup> The same two time-scale theory underpins the analysis of Hinderer and Flanagan [17], but this explicitly ignores resonances.

<sup>7</sup> In effect we are defining  $\omega(\tilde{\lambda}) \equiv \omega[J(\tilde{\lambda})]$ .

In the limit of  $\eta \rightarrow 0$  we are left with a constant frequency  $\omega_0(0)$ . The higher order terms are identified below by matching terms in the series expansions of the equations of motion. Taking the two time-scales as independent, we may write the time derivative to  $\mathcal{O}(\eta)$  as

$$\frac{d}{d\lambda} = \omega_0 \frac{\partial}{\partial \Psi} + \eta \omega_1 \frac{\partial}{\partial \Psi} + \eta \frac{\partial}{\partial \tilde{\lambda}}. \quad (\text{A8})$$

$$\omega_0 + \eta \omega_1 + \eta \frac{\partial q_0}{\partial \tilde{\lambda}} + \eta \omega_0 \frac{\partial q_1}{\partial \Psi} = \omega(J_0) + \eta \frac{d\omega}{dJ} J_1 + \eta \sum_s g_s^{(1)}(J_0) \exp[is(\Psi + q_0)], \quad (\text{A9a})$$

$$\eta \frac{\partial J_0}{\partial \tilde{\lambda}} + \eta \omega_0 \frac{\partial J_1}{\partial \Psi} = \eta \sum_s G_s^{(1)}(J_0) \exp[is(\Psi + q_0)]. \quad (\text{A9b})$$

Averaging (A9b) over  $\Psi$  gives<sup>8</sup>

$$\frac{\partial J_0}{\partial \tilde{\lambda}} = G_0^{(1)}(J_0). \quad (\text{A10})$$

This describes the adiabatic evolution, hence we can identify  $J_0(\tilde{\lambda})$  with (the lowest order piece of) the adiabatic solution [17]. If we similarly average (A9a) we find

$$\omega_0 + \eta \omega_1 + \eta \frac{\partial q_0}{\partial \tilde{\lambda}} = \omega(J_0) + \eta \frac{\partial \omega}{\partial J} \langle J_1 \rangle_\Psi + \eta g_0^{(1)}(J_0). \quad (\text{A11})$$

From this we can identify the terms that originate from the frequency and, matching by order in  $\eta$ , obtain

$$\omega_0 = \omega(J_0), \quad (\text{A12a})$$

$$\omega_1 = \frac{\partial \omega}{\partial J} \langle J_1 \rangle_\Psi. \quad (\text{A12b})$$

This leaves

$$\frac{\partial q_0}{\partial \tilde{\lambda}} = g_0^{(1)}(J_0), \quad (\text{A13})$$

$$q_0 = \kappa_0 + \int_0^{\tilde{\lambda}} g_0^{(1)}[J_0(\tau)] d\tau. \quad (\text{A14})$$

We now have expressions for the lowest order terms in the expansions.

Subtracting the  $s = 0$  components from (A9b) leaves

$$\omega_0 \frac{\partial J_1}{\partial \Psi} = \sum_{s \neq 0} G_s^{(1)}(J_0) \exp[is(\Psi + q_0)]. \quad (\text{A15})$$

This can be solved to give

$$J_1 = \langle J_1 \rangle_\Psi + \frac{1}{\omega_0} \sum_{s \neq 0} \frac{G_s^{(1)}(J_0) \exp[is(\Psi + q_0)]}{is}. \quad (\text{A16})$$

Using the two time-scale decomposition to replace the time derivatives in the equations of motion, and substituting in the ansatz expansions gives, to first order,

We can do the same for (A9a) to obtain

$$q_1 = \langle q_1 \rangle_\Psi + \frac{1}{\omega_0} \sum_{s \neq 0} \frac{g_s^{(1)}(J_0) \exp[is(\Psi + q_0)]}{is}. \quad (\text{A17})$$

To find the constants of integration,  $\langle q_1 \rangle_\Psi$  and  $\langle J_1 \rangle_\Psi$ , it is necessary to extend the analysis to second order in  $\eta$ . This shows that  $\langle J_1 \rangle_\Psi$  is the first-order component of the adiabatic solution. We do not need explicit forms for later calculations, so we will not proceed further. We have successfully constructed the pre-resonance solution.

## 2. Solution near resonance

Near to resonance, we consider an interior layer expansion [40]. As explained in Sec. IV A, evolution near resonance proceeds on a time-scale intermediate between the slow and fast times. We therefore introduce a rescaled time

$$\hat{\lambda} = \frac{\tilde{\lambda} - \tilde{\lambda}_*}{\eta^{1/2}} = \eta^{1/2}(\lambda - \lambda_*). \quad (\text{A18})$$

As for the before resonance solution, we can create a series expansion; however, now we expand in terms of  $\eta^{1/2}$  [12]

$$q(\hat{\lambda}; \eta) = \hat{q}_0(\hat{\lambda}) + \eta^{1/2} \hat{q}_{1/2}(\hat{\lambda}) + \mathcal{O}(\eta), \quad (\text{A19a})$$

$$J(\hat{\lambda}; \eta) = \hat{J}_0 + \eta^{1/2} \hat{J}_1(\hat{\lambda}) + \mathcal{O}(\eta). \quad (\text{A19b})$$

The series expansion for the frequency, (A2), can be rewritten as

$$\omega(\hat{\lambda}) = \eta^{1/2} \varpi_1 \hat{\lambda} + \eta \varpi_2 \hat{\lambda}^2 + \mathcal{O}(\eta^{3/2}). \quad (\text{A20})$$

<sup>8</sup> The ansatz is constructed such that  $J_0 \equiv \langle J_0 \rangle_\Psi$  and  $q_0 \equiv \langle q_0 \rangle_\Psi$ .



Proceeding to write the equations of motion in terms of the rescaled time gives

$$\begin{aligned} \frac{dq}{d\hat{\lambda}} &= \varpi_1 \hat{\lambda} + \eta^{1/2} \varpi_2 \hat{\lambda}^2 \\ &+ \eta^{1/2} \sum_s g_s^{(1)} \left( \hat{J}_0, \tilde{\lambda}_* \right) \exp(is\hat{q}_0) + \mathcal{O}(\eta), \end{aligned} \quad (\text{A21a})$$

$$\frac{dJ}{d\hat{\lambda}} = \eta^{1/2} \sum_s G_s^{(1)} \left( \hat{J}_0, \tilde{\lambda}_* \right) \exp(is\hat{q}_0) + \mathcal{O}(\eta). \quad (\text{A21b})$$

From the equations of motion we can match terms by their order in  $\eta^{1/2}$ . At zeroth order we find

$$\hat{J}_0 = \hat{\varrho}_0 \quad (\text{A22})$$

is constant, and

$$\hat{q}_0 = \hat{\kappa}_0 + \frac{\varpi_1 \hat{\lambda}^2}{2}. \quad (\text{A23})$$

Using these, we can build the next order terms

$$\begin{aligned} \hat{q}_{1/2} &= \hat{\kappa}_{1/2} + \frac{\varpi_2 \hat{\lambda}^3}{3} + g_0^{(1)}(\hat{\varrho}_0) \hat{\lambda} \\ &+ \sum_{s \neq 0} g_s^{(1)}(\hat{\varrho}_0) \exp(is\hat{\kappa}_0) \int_0^{\hat{\lambda}} \exp\left(\frac{is\varpi_1 \tau^2}{2}\right) d\tau, \end{aligned} \quad (\text{A24})$$

$$\begin{aligned} \hat{J}_{1/2} &= \hat{\varrho}_{1/2} + G_0^{(1)}(\hat{\varrho}_0) \hat{\lambda} \\ &+ \sum_{s \neq 0} G_s^{(1)}(\hat{\varrho}_0) \exp(is\hat{\kappa}_0) \int_0^{\hat{\lambda}} \exp\left(\frac{is\varpi_1 \tau^2}{2}\right) d\tau. \end{aligned} \quad (\text{A25})$$

Both of these involve the complex Fresnel integral [41], the details of which are given in the following section. We have now constructed the interior solution.

### 3. The complex Fresnel integral

The solution for the motion in the interior region near to resonance involves the integral

$$W(\hat{\lambda}) = \int_0^{\hat{\lambda}} \exp\left(\frac{is\varpi_1 \tau^2}{2}\right) d\tau. \quad (\text{A26})$$

The complex Fresnel integral is

$$\mathcal{Y}(z) = \int_0^z \exp\left(\frac{i\pi x^2}{2}\right) dx = \mathcal{C}(z) + i\mathcal{S}(z), \quad (\text{A27})$$

where  $\mathcal{C}(z)$  and  $\mathcal{S}(z)$  are the cosine and sine Fresnel integrals [41], and hence

$$W(\hat{\lambda}) = \sqrt{\frac{\pi}{s\varpi_1}} \mathcal{Y}\left(\sqrt{\frac{s\varpi_1}{\pi}} \hat{\lambda}\right). \quad (\text{A28})$$

We shall be interested in the asymptotic behaviour for  $|\hat{\lambda}| \rightarrow \infty$ . The complex Fresnel integral has the limit [41]

$$\lim_{|z| \rightarrow \infty} \mathcal{Y}(z) \sim \frac{\text{sgn } z}{\sqrt{2}} \exp\left(\frac{i\pi}{4}\right) - \frac{i}{\pi z} \exp\left(-\frac{i\pi z^2}{2}\right), \quad (\text{A29})$$

where

$$\text{sgn } z = \begin{cases} 1 & z > 0 \\ -1 & z < 0 \end{cases}. \quad (\text{A30})$$

Hence,

$$\begin{aligned} \lim_{|\hat{\lambda}| \rightarrow \infty} W(\hat{\lambda}) &\sim \frac{\text{sgn } \hat{\lambda}}{\sqrt{2}} \sqrt{\frac{\pi}{|s\varpi_1|}} \exp\left[\text{sgn}(s\varpi_1) \frac{i\pi}{4}\right] \\ &+ \frac{1}{is\varpi_1} \exp\left(\frac{is\varpi_1 \hat{\lambda}^2}{2}\right). \end{aligned} \quad (\text{A31})$$

### 4. Matching solutions

To complete our solution we must match the pre-resonance solution of Sec. A 1 with the near resonance solution of Sec. A 2. This is achieved by rewriting the pre-resonance solution in terms of the rescaled time  $\hat{\lambda}$  and comparing this with the near resonance solution expanded in the limit of  $\hat{\lambda} \rightarrow -\infty$ .

To rewrite the pre-resonance solution, we begin with the fast phase parameter

$$\Psi(\hat{\lambda}) = \frac{\Psi_*}{\eta} + \frac{\varpi_1 \hat{\lambda}^2}{2} + \eta^{1/2} \frac{\varpi_2 \hat{\lambda}^3}{3} + \mathcal{O}(\eta). \quad (\text{A32})$$

Using this together with equations (A14) and (A17) in (A6a), the angle variable is

$$q(\hat{\lambda}; \eta) = \frac{\Psi_*}{\eta} + \frac{\varpi_1 \hat{\lambda}^2}{2} + \kappa_* + \eta^{1/2} \frac{\varpi_2 \hat{\lambda}^3}{3} + \eta^{1/2} g_0^{(1)}(J_*) \hat{\lambda} + \frac{\eta^{1/2}}{\varpi_1 \hat{\lambda}} \sum_{s \neq 0} \frac{1}{is} g_s^{(1)}(J_*) \exp\left[is\left(\frac{\Psi_*}{\eta} + \frac{\varpi_1 \hat{\lambda}^2}{2} + \kappa_*\right)\right] + \mathcal{O}(\eta), \quad (\text{A33})$$

where we have defined  $J_* \equiv J_0(\tilde{\lambda}_*)$  and  $\kappa_* = \kappa_0 + \int_0^{\tilde{\lambda}_*} g_0^{(1)}[J_0(\tau)] d\tau$ , and used (A20) to substitute for  $\omega$ . The action

variable is similarly determined by using equations (A10) and (A16) with (A6b) to give

$$J(\hat{\lambda}; \eta) = J_\star + \eta^{1/2} G_0^{(1)}(J_\star) \hat{\lambda} + \frac{\eta^{1/2}}{\varpi_1 \hat{\lambda}} \sum_{s \neq 0} \frac{1}{is} G_s^{(1)}(J_\star) \exp \left[ is \left( \frac{\Psi_\star}{\eta} + \frac{\varpi_1 \hat{\lambda}^2}{2} + \kappa_\star \right) \right] + \mathcal{O}(\eta). \quad (\text{A34})$$

We can now compare this to the near resonance expansion with the integral replaced by the limiting form given in (A31).

At zeroth order, we immediately obtain

$$\hat{\kappa}_0 = \frac{\Psi_\star}{\eta} + \kappa_\star, \quad (\text{A35})$$

$$\hat{\varrho}_0 = J_\star. \quad (\text{A36})$$

These fix the integration constants. The more interesting result is now found by comparing the  $\mathcal{O}(\eta^{1/2})$  terms. Equating the angle variable expressions and cancelling terms gives

$$\hat{\kappa}_{1/2} = \sum_{s \neq 0} g_s^{(1)}(\hat{\varrho}_0) \sqrt{\frac{\pi}{2|s\varpi_1|}} \exp \left[ i \left( s\hat{\kappa}_0 + \frac{\pi}{4} \text{sgn } s\varpi_1 \right) \right]. \quad (\text{A37})$$

Similarly, for the action variables

$$\hat{\varrho}_{1/2} = \sum_{s \neq 0} G_s^{(1)}(\hat{\varrho}_0) \sqrt{\frac{\pi}{2|s\varpi_1|}} \exp \left[ i \left( s\hat{\kappa}_0 + \frac{\pi}{4} \text{sgn } s\varpi_1 \right) \right]. \quad (\text{A38})$$

We now have a matched solution through resonance.

Having constructed the solution, we see that the lowest order evolution corresponds to the adiabatic solution; the deviations come in at the following order. When we switch from the pre-resonance solution to the post-resonance solution, there is a change in the sign of  $\hat{\lambda}$ . Therefore, when matching the post-resonance solution  $\hat{\varrho}_{1/2}$  and  $\hat{\kappa}_{1/2}$  also change sign: there is a change of

$$\Delta q = 2\eta^{1/2} \hat{\kappa}_{1/2}, \quad (\text{A39})$$

$$\Delta J = 2\eta^{1/2} \hat{\varrho}_{1/2} \quad (\text{A40})$$

across the resonance [38]. We are not particularly interested in the deviation in  $J$ , of greater concern is the change in the orbital parameters  $\{E, L_z, Q\}$ . Assuming that there is a smooth transformation that maps between  $J$  and these, then, to lowest order, we can calculate the deviation relative to the adiabatic prescription by substituting the forcing functions  $G^{(1)} \rightarrow G_a^{(1)}$ , where  $G_a^{(1)}$

describes the evolution of  $\mathcal{I}_a$  through the effects of the self-force. This result is quoted by Flanagan and Hinderer [12]. The change in the orbital parameters is determined by the forcing functions, hence it is essential to have an accurate self-force model.

As a final step in understanding our result, we switch from Mino time to coordinate time. An appropriate redefinition of the forcing functions can be done by scaling by  $\Gamma$ , we define

$$F_a^{(1)} = \frac{G_a^{(1)}}{\Gamma}, \quad (\text{A41})$$

such that the equation of motion becomes

$$\left\langle \frac{d\mathcal{I}_a}{dt} \right\rangle_{q'} = \eta \sum_s F_{a,s}^{(1)}(\mathcal{I}) \exp(isq) + \mathcal{O}(\eta^2). \quad (\text{A42})$$

Here we have made the averaging over  $q'$  explicit to show that the equation is only defined as an orbital average: not only does our asymptotic expansion average out oscillations over an orbit in  $q'$ , but in converting from  $\lambda$  to  $t$  we have used  $\Gamma$  which is an orbital average. From (A2), we recognise that

$$\varpi_1 = \frac{\partial \omega}{\partial \hat{\lambda}} = \frac{\Gamma^2}{\eta} \left\langle \dot{\Omega} \right\rangle_{q'}. \quad (\text{A43})$$

We have used the averaged form of  $\dot{\Omega}(t)$  as this is appropriate. Using these to adapt equations (A38) and (A40), we obtain

$$\begin{aligned} \Delta \mathcal{I}_a &= \eta \sum_{s \neq 0} F_{a,s}^{(1)}(\mathcal{I}_\star) \sqrt{\frac{2\pi}{|s\langle \dot{\Omega} \rangle_{q'}|}} \\ &\quad \times \exp \left[ i \left( s\hat{\kappa}_0 + \frac{\pi}{4} \text{sgn } s\langle \dot{\Omega} \rangle_{q'} \right) \right] \end{aligned} \quad (\text{A44})$$

$$= \eta \sum_{s \neq 0} F_{a,s}^{(1)}(\mathcal{I}_\star) \tau_{\text{res},s} \exp \left[ i \left( s\hat{\kappa}_0 + \frac{\pi}{4} \text{sgn } s\langle \dot{\Omega} \rangle_{q'} \right) \right], \quad (\text{A45})$$

using (28) and representing the values on resonance of  $E$ ,  $L_z$  and  $Q$  with  $\mathcal{I}_\star$ .

- 
- [1] S. Chandrasekhar, *The Mathematical Theory of Black Holes*, Oxford Classic Texts in the Physical Sciences (Oxford University Press, Oxford, 1992).  
 [2] F. Pretorius, Physical Review Letters, **95**, 121101 (2005),

- arXiv:0507014 [gr-qc].  
 [3] M. Campanelli, C. O. Lousto, P. Marronetti, and Y. Zlochower, Physical Review Letters, **96**, 111101 (2006), arXiv:0511048 [gr-qc].

- [4] J. G. Baker, J. Centrella, D.-I. Choi, M. Koppitz, and J. van Meter, *Physical Review Letters*, **96**, 111102 (2006), arXiv:0511103 [gr-qc].
- [5] G. M. Harry, *Classical and Quantum Gravity*, **27**, 084006 (2010).
- [6] T. Accadia et al., *Classical and Quantum Gravity*, **28**, 114002 (2011).
- [7] K. Kuroda, *Classical and Quantum Gravity*, **27**, 084004 (2010).
- [8] P. Amaro-Seoane et al., *Classical and Quantum Gravity*, **29**, 124016 (2012), arXiv:1202.0839.
- [9] P. Amaro-Seoane, J. R. Gair, M. Freitag, M. C. Miller, I. Mandel, C. J. Cutler, and S. Babak, *Classical and Quantum Gravity*, **24**, R113 (2007), arXiv:0703495 [astro-ph].
- [10] L. Barack, *Classical and Quantum Gravity*, **26**, 213001 (2009), arXiv:0908.1664.
- [11] E. Poisson, *Living Reviews in Relativity*, **7** (2004), doi: 10.12942/lrr-2004-6, arXiv:0306052 [gr-qc].
- [12] É. É. Flanagan and T. Hinderer, *Physical Review Letters*, **109**, 071102 (2012), arXiv:1009.4923.
- [13] H. Goldstein, C. Poole, and J. Safko, *Classical Mechanics*, 3rd ed. (Pearson Education International, Upper Saddle River, New Jersey, 2002).
- [14] A. Pound and E. Poisson, *Physical Review D*, **77**, 044013(18) (2008), arXiv:0708.3033.
- [15] J. R. Gair, É. É. Flanagan, S. Drasco, T. Hinderer, and S. Babak, *Physical Review D*, **83**, 044037 (2011), arXiv:1012.5111.
- [16] E. E. Flanagan, S. A. Hughes, and U. Ruangsri, *Physical Review D*, **85**, 22 (2012), arXiv:1208.3906.
- [17] T. Hinderer and É. É. Flanagan, *Physical Review D*, **78**, 064028 (2008), arXiv:0805.3337.
- [18] B. Carter, *Physical Review*, **174**, 1559 (1968).
- [19] Y. Mino, *Physical Review D*, **67**, 084027 (2003), arXiv:0302075 [gr-qc].
- [20] S. Drasco, É. É. Flanagan, and S. A. Hughes, *Classical and Quantum Gravity*, **22**, S801 (2005), arXiv:0505075 [gr-qc].
- [21] V. I. Arnold, V. Kozlov, and A. I. Neishtadt, in *Dynamical Systems III*, Encyclopaedia of Mathematical Sciences, edited by V. I. Arnold (Springer-Verlag, New York, 1988).
- [22] R. Grossman, J. Levin, and G. Perez-Giz, *Physical Review D*, **85**, 023012 (2012), arXiv:1105.5811.
- [23] D. Wilkins, *Physical Review D*, **5**, 814 (1972).
- [24] C. Darwin, *Proceedings of the Royal Society A: Mathematical, Physical and Engineering Sciences*, **263**, 39 (1961).
- [25] S. Drasco and S. Hughes, *Physical Review D*, **69**, 044015 (2004), arXiv:0308479 [astro-ph].
- [26] S. Hughes, *Physical Review D*, **61**, 084004 (2000), arXiv:9910091 [gr-qc].
- [27] W. Schmidt, *Classical and Quantum Gravity*, **19**, 2743 (2002), arXiv:0202090 [gr-qc].
- [28] F. D. Ryan, *Physical Review D*, **53**, 3064 (1996).
- [29] K. Glampedakis, S. Hughes, and D. Kennefick, *Physical Review D*, **66**, 064005 (2002), arXiv:0205033 [gr-qc].
- [30] D. L. Bosley and J. Kevorkian, *SIAM Journal on Applied Mathematics*, **52**, 494 (1992).
- [31] N. Warburton, S. Akcay, L. Barack, J. R. Gair, and N. Sago, *Physical Review D*, **85**, 061501(R) (2012), arXiv:1111.6908.
- [32] V. I. Arnol'd, *Russian Mathematical Surveys*, **18**, 9 (1963).
- [33] J. Moser, *Stable and Random Motions in Dynamical Systems: With Special Emphasis on Celestial Mechanics*, Annals of mathematical studies (Princeton University Press, Princeton, New Jersey, 1973).
- [34] É. É. Flanagan and T. Hinderer, *Physical Review D*, **75**, 124007 (2007), arXiv:0704.0389.
- [35] B. R. Iyer and C. M. Will, *Physical Review Letters*, **70**, 113 (1993).
- [36] L. E. Kidder, *Physical Review D*, **52**, 821 (1995), arXiv:9506022 [gr-qc].
- [37] J. Brink, M. Geyer, and T. Hinderer, *Physical Review D*, **87**, 5 (2013), arXiv:1304.0330.
- [38] J. Kevorkian, *SIAM Review*, **29**, 391 (1987).
- [39] J. Gair, N. Yunes, and C. M. Bender, *Journal of Mathematical Physics*, **53**, 032503 (2012), arXiv:1111.3605.
- [40] J. Kevorkian, *SIAM Journal on Applied Mathematics*, **20**, 364 (1971).
- [41] F. W. J. Olver, W. Lozier, Daniel, R. F. Boisvert, and C. W. Clark, eds., *NIST Handbook of Mathematical Functions* (Cambridge University Press, Cambridge, 2010).